

© 2025 by the author(s).

This work is licensed under Creative Commons Attribution 4.0 International License
<https://creativecommons.org/licenses/by/4.0/>



How to cite: Lohvyniuk H, Husak Ye, Vynnychenko I, Solodovnyk O. Comparative analysis of bone healing under physiological and trace element overload conditions in senile rats. *East Ukr Med J.* 2025;13(3):723-733

DOI: [https://doi.org/10.21272/eumj.2025;13\(3\):723-733](https://doi.org/10.21272/eumj.2025;13(3):723-733)

ABSTRACT

Hanna Lohvyniuk

<https://orcid.org/0000-0002-4635-2322>

Sumy State University, Department of Oncology and Radiology, Sumy, Ukraine;

Yevheniia Husak

<https://orcid.org/0000-0002-2217-3717>

Silesian University of Technology, Faculty of Chemistry, Gliwice, Poland; Sumy State University, Biomedical Research Centre, Sumy, Ukraine

Ihor Vynnychenko

<https://orcid.org/0000-0002-2339-6509>

Sumy State University, Department of Oncology and Radiology, Sumy, Ukraine;

Oleksandr Solodovnyk

<https://orcid.org/0000-0003-2785-5175>

Sumy State University, Department of Surgery, Traumatology, Orthopedics and Phthisiology, Sumy, Ukraine

COMPARATIVE ANALYSIS OF BONE HEALING UNDER PHYSIOLOGICAL AND TRACE ELEMENT OVERLOAD CONDITIONS IN SENILE RATS

Introduction. Age-related impairment of bone healing is a growing clinical concern. While the role of trace elements in bone metabolism is well recognized, their effect on cancellous bone regeneration in elderly organisms remains poorly understood. Our study contributes a valuable foundation for understanding how excess exposure to specific trace elements – namely zinc (Zn), manganese (Mn), copper (Cu), lead (Pb), and chromium (Cr) – affects bone regeneration. Through a comparative histological and ultrastructural analysis of fracture healing in control and microelement-overload groups, we aim to elucidate the mechanisms by which trace elements modulate bone repair, angiogenesis, and osteogenesis in aged organisms.

Methods. Our study was focused on comparing the course of cancellous bone healing under physiological conditions and trace element overconsumption in senile rats using histological and scanning electron microscopy analysis.

Results. The results showed cancellous bone healing of control group followed a time-dependent sequence of inflammation, granulation tissue formation, fibroreticular remodeling, and coarse woven bone deposition. In contrast, the trace element overconsumption group exhibited delayed and disorganized reparative osteogenesis, marked by delay tissue formation, prolonged inflammatory features, and substantial cartilaginous tissue formation by day 21. Reduced vascular density in MeG animals suggested impaired angiogenesis, further contributing to compromised regeneration.

Conclusions. Trace element overconsumption alters the normal trajectory of cancellous bone healing in senile rats, inducing a shift toward endochondral ossification and impairing vascularization. These findings underscore the critical influence of microelement balance on skeletal repair in aging organisms.

Keywords: reparative osteogenesis, microelementosis, cancellous bone tissue, senile rat.

Corresponding author: Yevheniia Husak, Silesian University of Technology, Faculty of Chemistry, Gliwice, Poland
e-mail: evgenia.husak@gmail.com

РЕЗЮМЕ

Ганна Логвинюк
<https://orcid.org/0000-0002-4635-2322>
Сумський державний університет,
кафедри онкології та радіології, Суми,
Україна

Євгенія Гусак
<https://orcid.org/0000-0002-2217-3717>
Сілезький технологічний
університет, Хімічний факультет,
Глівіце, Польща;
Сумський державний університет,
Центр біомедичних досліджень,
Суми, Україна

Ігор Винниченко
<https://orcid.org/0000-0002-2339-6509>
Сумський державний університет,
кафедра онкології та радіології,
Суми, Україна

Олександр Солодовник
<https://orcid.org/0000-0003-2785-5175>
Сумський державний університет,
кафедра хірургії, травматології,
ортопедії та фізйотрії, Суми, Україна

ПОРІВНЯЛЬНИЙ АНАЛІЗ ПРОЦЕСІВ ЗАГОЄННЯ КІСТКОВОЇ ТКАНИНИ ЗА ФІЗІОЛОГІЧНИХ УМОВ І УМОВ НАДМІРНОГО НАДХОДЖЕННЯ МІКРОЕЛЕМЕНТІВ У СТАРИХ ЩУРІВ

Вступ. Вікове порушення загоєння кісткової тканини є зростаючою клінічною проблемою. Хоча роль мікроелементів у метаболізмі кісткової тканини є добре вивченою, їхній вплив на регенерацію губчастої кістки в організмах літнього віку залишається недостатньо з'ясованою.

Методи. У цьому дослідженні було проведено порівняльний аналіз динаміки загоєння губчастої кісткової тканини у старих щурів за фізіологічних умов та за умов надлишкового споживання мікроелементів із використанням гістологічного та скануючого електронномікроскопічного аналізу.

Результати. У контрольній групі процес регенерації відбувався згідно загально визнаним етапам репаративного остеогенезу: запалення, формування грануляційної тканини, розвиток фіброретикулярної тканини та відкладення грубоволокнистої кісткової тканини. На відміну від цього, у групі з надмірним надходженням мікроелементів спостерігався уповільнений та дезорганізований репаративний остеогенез, що проявлявся затримкою формування тканин, тривалим запаленням та значною кількістю хрящової тканини на 21-шу добу. Зменшення щільності судин у тварин цієї групи свідчило про порушення ангиогенезу, що додатково ускладнило процес регенерації.

Висновки. Надмірне споживання мікроелементів змінило нормальний хід загоєння губчастої кісткової тканини у тварин старечої групи, сприяючи переходу до хрящового остеогенезу та порушенню ангиогенезу. Отримані результати підкреслюють критичну важливість мікроелементного балансу для ефективного відновлення кісткової тканини в умовах старіння організму.

Ключові слова: репаративний остеогенез, мікроелементоз, губчаста кісткова тканина, щури старечого віку.

Автор, відповідальний за листування: Євгенія Гусак, Сілезький технологічний університет, Хімічний факультет, Глівіце, Польща
e-mail: evgenia.husak@gmail.com

ABBREVIATIONS

BMD – bone mineral density,
CG – control group,

H&E – hematoxylin and eosin,
MeG – experimental groups,
SEM – scanning electron microscopy

INTRODUCTION

Bone is a highly mineralized connective tissue characterized by an intercellular matrix enriched with inorganic components, primarily in the form of

hydroxyapatite crystals [1]. Previous studies have demonstrated correlations between trace element concentrations within the human exposome – encompassing dietary intake, drinking water, and

airborne particulates – and their subsequent accumulation in bone mineral matrices [2]. Metabolic factors, environmental exposure, and nutritional status contribute significantly to the development of bone diseases and pathologies, including fractures and osteonecrosis. Variations in specific trace element levels have been associated with compromised bone integrity and impaired regenerative capacity [3].

The number of elderly individuals suffering from bone-related diseases continues to rise due to demographic shifts and increased life expectancy. Musculoskeletal disorders are among the most widespread noncommunicable diseases globally, with osteoporosis and osteoarthritis being the most prevalent in aging populations [3, 4]. Among the diverse factors influencing bone metabolism, trace elements have attracted growing scientific attention due to their dual role: they may exert osteoprotective effects when present at optimal levels or induce toxicity when deficient or in excess. Proper trace element balance is essential for maintaining bone homeostasis, and both deficiency and overload may lead to metabolic bone diseases and delayed fracture healing [5].

Essential elements such as zinc, copper, manganese contribute to enzymatic functions, collagen synthesis, osteoblastic activity, and antioxidative defense mechanisms [6, 7]. Conversely, heavy metals such as lead and cadmium disrupt cellular processes, inhibit osteogenic differentiation, and induce oxidative stress, thereby compromising skeletal integrity [7, 8]. Moreover, a growing body of evidence highlights the pivotal role of trace elements in maintaining bone health by modulating bone mineral density (BMD), lowering fracture risk, and preventing degenerative skeletal disorders [9, 10]. These microelements are involved in complex biochemical pathways that regulate inflammation, vascularization, and cell signaling essential for bone regeneration. Studies have shown that trace elements influence the function of osteoblasts, osteoclasts, chondrocytes, and endothelial cells—key players in bone remodeling and repair [11]. For instance, Dr. Pasco and Dr. Han explored the impact of dietary copper intakes on BMD, demonstrating their relevance in maintaining bone architecture in aging individuals [9]. Another notable study by Martínez-Nava and colleagues investigated the role of cadmium that cadmium exposure may influence negatively the level of essential elements, such as zinc, iron, manganese [12]. Although these studies highlight diverse molecular mechanisms through which trace elements influence skeletal biology, nevertheless, despite growing insights, many underlying regulatory pathways remain incompletely understood, necessitating continued research to develop targeted therapeutic strategies [9], [13].

One of the least explored areas pertains to the dynamics of cancellous (spongy) bone healing under varying conditions of trace element exposure. The literature currently lacks robust experimental data on how different microelements influence the regenerative processes following trabecular bone fractures, particularly in elderly organisms [14]. This knowledge gap is critical given the increasing incidence of such fractures and the complex interplay of aging-related physiological decline and bone metabolism.

Moreover, most existing experimental models fail to adequately replicate the aged bone environment or account for trace element imbalances. To address this gap, the present study employs an *in vivo* model [15] designed to investigate cancellous bone healing in senile rats under both physiological and microelement-overload conditions. This approach, developed by our colleagues, incorporates a combination of several trace elements and evaluates their long-term effects. The complex interplay among these elements may result in synergistic or antagonistic outcomes. By replicating the pathophysiological context of age-related microelementosis, the study aims to provide clinically relevant insights into reparative osteogenesis in the elderly.

This research is particularly timely given the limited number of comprehensive animal studies in this domain and the technical challenges involved in reproducing cancellous bone fractures experimentally. Our study contributes a valuable foundation for understanding how excess exposure to specific trace elements – namely zinc (Zn), manganese (Mn), copper (Cu), lead (Pb), and chromium (Cr) – affects bone regeneration. Through a comparative histological and ultrastructural analysis of fracture healing in control and microelement-overload groups, we aim to elucidate the mechanisms by which trace elements modulate bone repair, angiogenesis, and osteogenesis in aged organisms [16].

MATERIALS AND METHODS

Design of animal experiments and surgical procedures

All animal procedures were approved by the Ethical Committee of Sumy State University (Protocol 12/07 from 14.07.2022) and conducted in accordance with the international principles outlined in the European Convention for the Protection of Vertebrate Animals Used for Experimental and Other Scientific Purposes (Strasbourg, 1986), as well as the national legislation of Ukraine, On the Protection of Animals from Cruel Treatment.

All animals included in the study were senile rats (aged 18–20 months), which represented the single age group. A total of 36 older male rats were used to evaluate a calcaneal fracture model (Figure 1). The model was

established by creating a transverse osteotomy in the calcaneal bone. Surgical procedures were carried out under general anesthesia induced by intraperitoneal injection of ketamine (50 mg/kg) and xylazine hydrochloride (10 mg/kg). To ensure aseptic conditions, the surgical site was sterilized with povidone-iodine. A standard lateral approach was employed to access the calcaneus, followed by bone stabilization. A critical-size segmental defect (1 mm) was created using a dental turbine/micromotor bur (\varnothing 1 mm) under continuous saline irrigation to prevent thermal damage. The animals were randomly assigned to control (CG) and experimental (MeG) groups and were sacrificed at three time points: days 7, 14, and 21 ($n = 6$ per group per time point). Euthanasia was performed under deep anesthesia

using an overdose of ketamine/xylazine to ensure that potential pain or distress was minimized. The last period of justification corresponds to the late phase of reparative osteogenesis in rats, during which both bone tissue formation and early signs of delayed healing or remodeling disturbances can be evaluated [17, 18]. One month prior to the surgical procedure and throughout the experimental period, the experimental group received an aqueous mixture of heavy metal salts at the following concentrations: $Zn^{2+} - 5$ mg/L, $Mn^{2+} - 0.1$ mg/L, $Cu^{2+} - 1$ mg/L, $Pb^{2+} - 0.1$ mg/L, and $Cr^{3+} - 0.1$ mg/L. At the end of each time point on 7th, 14th and 21st day, animals were euthanized via CO_2 asphyxiation, and the calcaneal samples were subjected to histological and scanning electron microscopy (SEM) analyses.

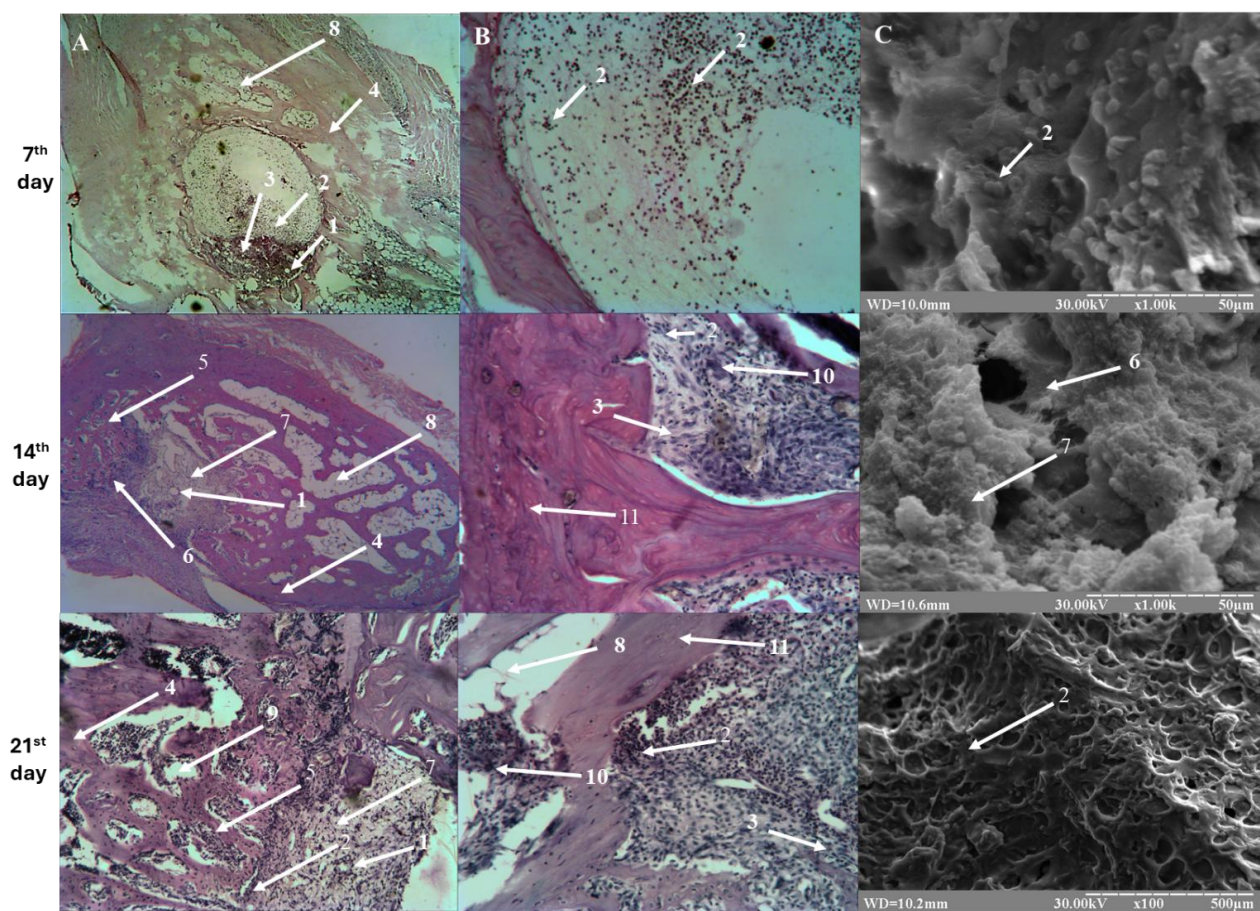


Figure 1. Histological (A, B) and scanning electron microscopy (SEM) (C) images illustrating the regenerative process of calcaneal bone defects in the control group of senile rats on 7–21 post-injury.

(A) Hematoxylin and eosin (H&E) staining at $\times 40$ magnification and (B) H&E staining at $\times 200$ magnification reveal the morphological features of the regenerate, including granulation and woven tissues, as well as the interface with native bone. (C) SEM image at $\times 1.00k - \times 100$ magnification provides ultrastructural visualization of the defect zone, highlighting the organization of newly formed bone and associated cellular and extracellular components.

Key structures identified: 1 – Capillaries, 2 – Lymphocytic cells, 3 – Fibroblast cells, 4 – Mature bone tissue, 5 – Coarse woven bone tissue, 6 – Fibroreticular tissue, 7 – Granulation tissue, 8 – Adipocytes, 9 – Bone marrow cavities, 10 – Macrophages cells, 11 – Osteocytic lacunae

Histological analysis

Calcaneal bones were fixed in 10% neutral buffered formalin for 24 hours. After fixation, the samples were decalcified in a formic acid solution under constant agitation for one week. The decalcified tissues were then dehydrated through a graded ethanol series and embedded in paraffin. Serial sections, 5–7 μm thick, were prepared using a microtome and stained with hematoxylin and eosin (H&E) to evaluate general tissue morphology. To quantify the formation of histological structures, three representative sections from each sample were analyzed using ImageJ software. The results were normalized to a standard area of one square millimeter. Additionally, the sizes of the formed structures were determined by measuring their diameters in each histological section.

Scanning Electron Microscope (SEM) imaging

Calcaneal bones were fixed in 5% glutaraldehyde for 24 hours, followed by dehydration in a graded ethanol series (50%, 70%, 80%, 90%, and 100%). The samples were then sectioned at the regeneration site and mounted on graphite tape. Surface coating with silver was performed using the VUP-5 sputter coater. The morphology of the regenerative process was examined using a RYeMMA-102 scanning electron microscope (SEMI OJSC, Sumy, Ukraine). SEM observations were interpreted in the context of adjacent histological sections stained with H&E.

Statistical analysis

Statistical analyses were performed using GraphPad Prism version 9. Results are presented as mean \pm standard deviation (SD), both numerically and graphically.

RESULTS

On the seventh day of reparative osteogenesis, histological analysis of the control group revealed that the regeneration zone was largely occupied by a dense inflammatory infiltrate, indicating the early phase of the

bone healing process (Figure 1). Numerous hemorrhagic foci and necrotic areas were present, particularly surrounding the fractured trabeculae, which appeared thinned, detached, and structurally compromised. The trabecular disintegration was likely due to both mechanical injury and osteoclastic resorption.

The cellular infiltrate was predominantly composed of lymphocytic cells, indicating acute inflammation. Granulation tissue had already begun to form, occupying $75.23 \pm 2.8\%$ of the regeneration zone, while a morphometric analysis of the defect area showed granulation tissue filled $70.65 \pm 1.61\%$ of the bone defect (Table 1). The granulation tissue consisted of loose connective stroma with immature fibroblasts and newly forming capillaries. In addition, adipocytic infiltration within the bone marrow cavities was noted, contributing to the thinning of trabeculae. This adipogenic replacement of hematopoietic elements is a known aging-related change that negatively affects osteogenesis [19]. Differentiation of mesenchymal stem cells into adipocytes leads to reduced osteoblastogenesis and stimulation of osteoclastogenesis. All these processes result in decreased formation of new bone tissue and predominance of resorption, which clearly explains the phenomenon of trabecular thinning in aging organisms [20, 21].

SEM provided further structural detail. The regenerating tissue at the interface between bone trabeculae and granulation tissue exhibited residual hemorrhagic traces, indicative of incomplete resorption of the post-traumatic hematoma. The regenerate appeared relatively homogeneous but immature, lacking definitive organization into woven or ossified components. These findings suggest that the healing process in aged animals proceeds at a slower pace, with delayed transition from inflammation to tissue remodeling.

Table 1. The morphometric parameters of bone defect in different time-points of regenerative process

Group	Days	Granulation, %	Fibroreticular, %	Coarse fiber, %	Lamellar bone, %	Average diameter vessels, μm	Average vascular area, μm^2	Average cavity area, μm^2
CG	7	70.65 \pm 1.61	–	–	–	2.97 \pm 0.42	3.66 \pm 0.62	167.70 \pm 55.19
	14	34.8 \pm 2.21	62.98 \pm 1.27	–	–	3.82 \pm 0.6	42.82 \pm 26.62	149.27 \pm 24.82
	21	15.10 \pm 1.13	22.17 \pm 1.16	62.97 \pm 1.93	–	4.2 \pm 0.82	10.8 \pm 3.07	179.61 \pm 28.09
Group	Days	Granulation, %	Fibroreticular, %	Coarse fiber, %	Cartilaginous tissue, %	Average diameter vessels, μm	Average vascular area, μm^2	Average cavity area, μm^2
MeG	7	–	–	–	–	–	–	303.95 \pm 95.76
	14	19.32 \pm 0.42	–	–	–	2.20 \pm 0.24	23.4 \pm 4.79	125.83 \pm 47.56
	21	–	45.76 \pm 0.47	13.6 \pm 0.31	32.37 \pm 0.74	2.38 \pm 0.28	11.52 \pm 1.065	187.7 \pm 35.36

By day 14 post-injury, the inflammatory infiltrate had fully subsided, as evidenced by the absence of inflammatory cells within the defect area. The central region of the regenerate was now dominated by granulation tissue ($34.8 \pm 2.21\%$), characterized by randomly oriented collagen fibers, immature mesenchymal cells, and angiogenic capillaries. Meanwhile, the peripheral zone transitioned into fibroreticular tissue, constituting $62.98 \pm 1.27\%$ of the regenerate. This tissue was denser and more organized, forming a meshwork that supported early osteoid deposition. Pronounced angiogenesis was observed within the regenerate's central portion, marked by dilated capillaries and developing sinusoids. In the periphery, there was evidence of active remodeling of maternal bone tissue, with osteocyte-populated trabeculae and adjacent proliferating osteoblasts contributing to new bone matrix formation. The cellular composition of the regenerate at this stage was highly polymorphic, including macrophages, reticulocytes, and fibroblasts, supporting ongoing tissue remodeling. Histological staining revealed homogeneous and intense osteoid deposition in the newly formed trabeculae, sharply contrasting with the older surrounding bone. However, some peripheral trabeculae showed empty osteocytic lacunae, a feature potentially indicating prior osteocyte apoptosis. Adipocytes were still abundant in the bone marrow cavities, reflecting ongoing senescence-associated changes.

By day 21, the regenerate exhibited advanced structural maturation. The central part of the defect was occupied by residual granulation tissue ($15.10 \pm 1.12\%$) and fibroreticular tissue ($22.17 \pm 1.16\%$), both of which had decreased compared to earlier stages. The granulation tissue still retained randomly oriented fibers and angiogenic profiles, suggesting that vascular remodeling persisted.

The most prominent feature at this stage was the development of coarse woven bone, which had become the predominant component ($62.97 \pm 1.93\%$) of the regenerate. This bone was organized into a fine-looped trabecular network and was structurally integrated with the maternal bone at the fracture margins. The woven bone tissue appeared intensely eosinophilic and homogeneous, consistent with woven bone formation. The cellular landscape was dominated by fibroblasts, macrophages, and lymphocytes, which are characteristic of the late remodeling phase. Residual tissue-filled cavities and persistent adipocytic infiltration were still observed, particularly in the bone marrow regions, indicating incomplete hematopoietic restoration. The newly formed trabeculae varied in density and osteoblast coverage, suggesting heterogeneous maturation of the

ossified regenerate. SEM imaging confirmed these findings, revealing a progressively organized regenerative architecture with visible trabecular scaffolds, reduced hemorrhagic debris, and improved bone-regenerate integration.

On the seventh day of reparative osteogenesis in the MeG group, the regenerative response was markedly delayed compared to the control (Figure 2). Histological analysis revealed well-demarcated fracture boundaries with limited signs of organized repair. The interfragmentary space was filled with a persistent blood clot, interwoven with fibrin strands and edematous cavities, indicating stalled hematoma resorption and inefficient transition to granulation tissue.

The surrounding trabecular bone was extensively damaged, showing signs of fissures, cracks, and delamination. Numerous trabeculae appeared thin and fragmented, and vast osteocyte-depleted areas were observed, reflecting widespread bone necrosis. Bone marrow cavities were dominated by adipocytes, a common hallmark of aging and disrupted hematopoiesis. SEM analysis confirmed these observations, revealing a structurally disorganized and heterogeneous regenerate surface, with accumulated hematoma, lymphocytic infiltration, and a lack of organized matrix deposition. The overall microarchitecture suggested minimal osteogenic activity, signifying that trace element overload impairs early-stage bone healing by delaying both inflammation resolution and regenerative signaling cascades.

By day 14, although reparative activity had initiated, the process remained markedly inferior to that in the control group. Notably, in the experimental animals the regenerate appeared even less organized than at day 7, reflecting a regression of healing dynamics under trace element overload. Granulation tissue was still the predominant component, accounting for $19.32 \pm 1.16\%$ of the regenerate (Table 1), and was largely restricted to the lower regions of the defect. The granulation matrix contained fibroblasts at different maturation stages and poorly differentiated stromal cells, indicating ongoing but incomplete cellular organization.

Persistent lymphocytic infiltration and residual blood clots highlighted a prolonged inflammatory phase. Engorged sinusoids and capillaries were present but appeared unevenly distributed, especially within the deeper granulation zones, suggesting impaired or inefficient angiogenesis. Small foci of bone marrow regeneration were noted in the intertrabecular spaces, though their appearance was sporadic and lacked structural integration.

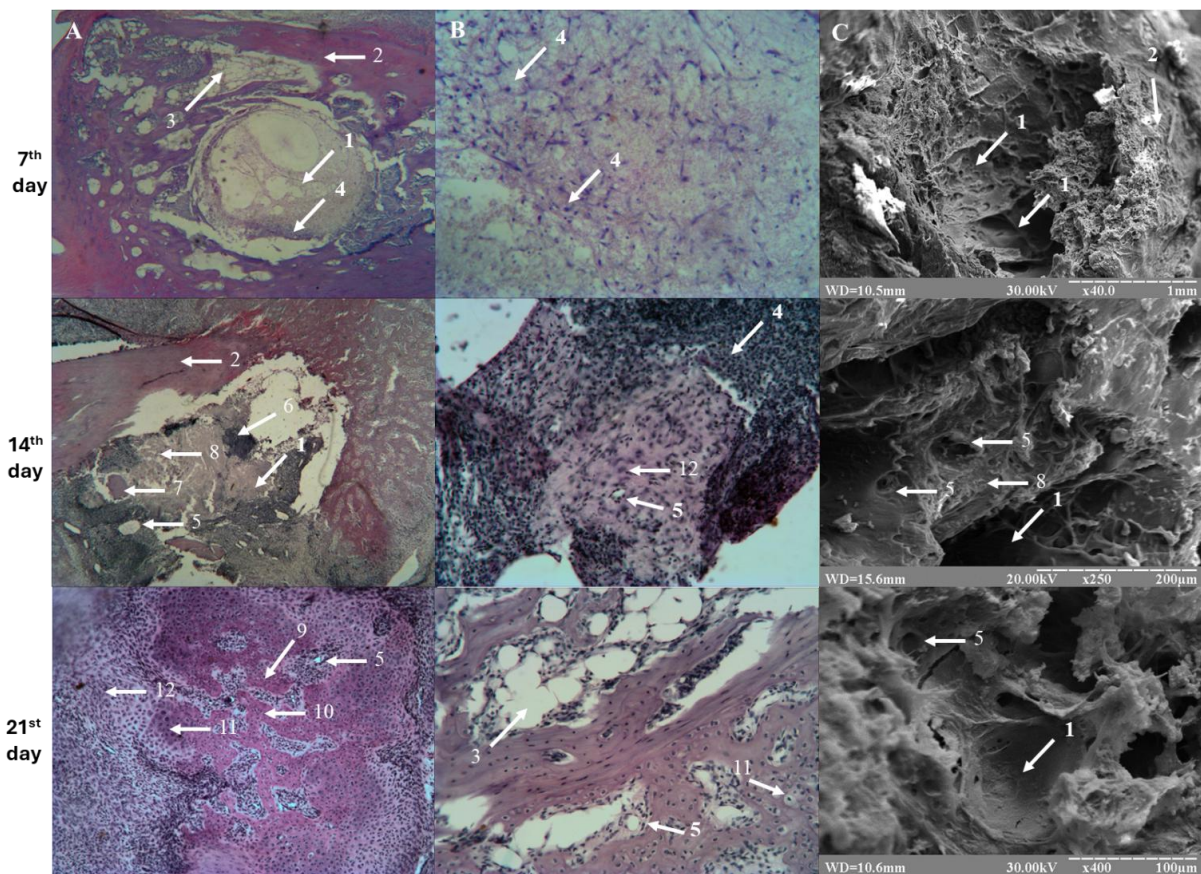


Figure 2. Histological (A) and scanning electron microscopy (SEM) (B) images of calcaneal bone defect regeneration in the experimental group (MeG) of senile rats under trace element overconsumption conditions.

(A) Hematoxylin and eosin (H&E) staining at $\times 40$ magnification and (B) H&E staining at $\times 200$ magnification highlight delayed tissue regeneration characterized by the presence of residual hematoma, lymphocytic infiltration, and incomplete granulation and fibroreticular matrix formation. Adipocyte accumulation and cartilaginous areas indicate impaired osteogenesis and a shift toward endochondral ossification. (C) SEM image at $\times 40$, $\times 250$ and $\times 400$ magnification shows an irregular regenerate surface with immature trabeculae, fragmented collagen fibers, and limited integration with the host bone.

Labeled structures: 1 – Regenerate zone, 2 – Bone tissue, 3 – Adipocytes, 4 – Lymphocytic cells, 5 – Capillaries, 6 – Lymphocytic infiltration, 7 – Residual hematoma, 8 – Granulation tissue, 9 – Fibroreticular tissue, 10 – Coarse woven bone tissue, 11 – Cartilage tissue, 12 – Collagen fibers

The peripheral bone tissue adjacent to the defect continued to exhibit significant structural compromise, with no clear signs of remodeling or new matrix deposition. Only sparse, flattened osteoblast-like cells were observed along limited trabecular surfaces, indicating minimal osteogenic activity and insufficient cellular support for robust osteoid synthesis. SEM imaging echoed these findings, visualizing a mosaic and poorly organized regenerate surface, dotted with engorged blood vessels, uneven collagen deposition, and limited evidence of osteoid formation.

On the twenty-first day, some degree of regenerative remodeling became apparent; however, the pattern differed fundamentally from the control (Figure 2, Figure 3 (B-D)). The regenerate now consisted of fibroreticular tissue ($45.76 \pm 2.4\%$), woven bone ($13.6 \pm$

1.175%), and cartilaginous tissue ($32.37 \pm 2.59\%$). This tissue composition clearly diverged from the control group, which lacked cartilaginous elements and demonstrated predominantly woven bone formation. In the MeG group, coarse woven bone and cartilage were distributed in a mosaic-like arrangement, especially in the deeper regions of the defect. This configuration suggests a partial shift toward endochondral ossification, likely as a compensatory mechanism triggered by impaired osteogenesis due to microelement imbalance. The fibroreticular component remained dense and randomly woven, with abundant fibroblasts but limited vascular structures. Tissue-filled cavities were still present, indicating delayed matrix consolidation.

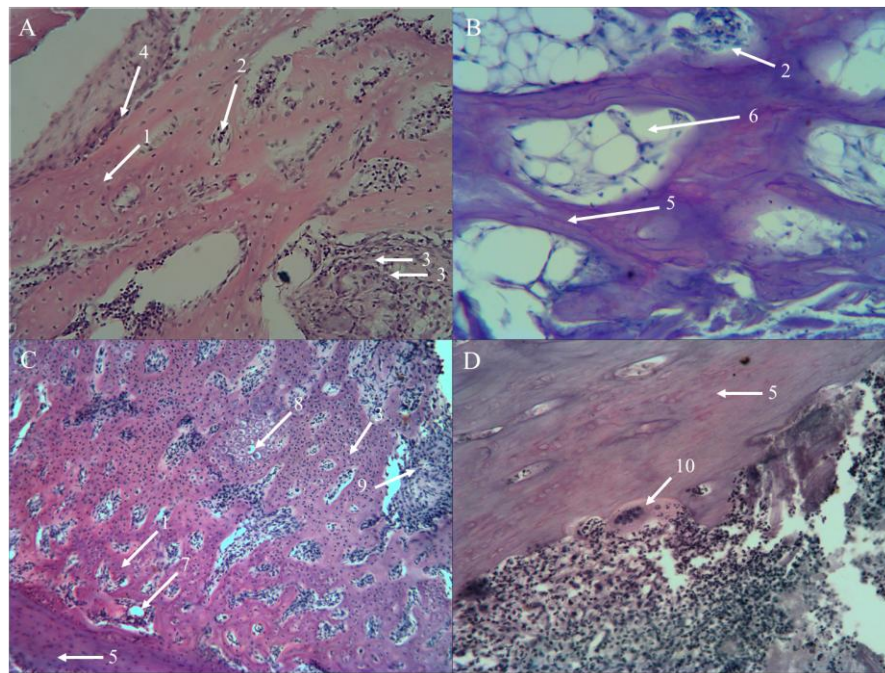


Figure 3. Histological microscopy images of calcaneal bone defect regeneration in senile rats, stained with hematoxylin and eosin (H&E), illustrating distinct histological structures: (A) control group on day 21, $\times 200$ magnification; (B–D) experimental group (MeG) under trace element overconsumption: (B) $\times 400$ magnification, (C) $\times 100$ magnification, (D) $\times 100$ magnification.

Labeled structures: 1 – fibrous bone tissue, 2 – bone marrow cavities, 3 – fibroreticular bone, 4 – osteoblast cells line, 5 – bone tissue, 6 – adipocytes, 7 – capillaries, 8 – cartilage tissue, 9 – collagen fibers, 10 – osteocytic lacunae

At the interface with the host bone, osteoblast layers were sparse and poorly defined. Resorptive lacunae and thinned trabeculae were common, and adipocyte-rich marrow remained dominant. The newly formed trabeculae in the center of the defect exhibited a fine-looped pattern, but with low osteoblast density and variable morphology – some elongated, others flattened or irregular – indicative of impaired osteoblast function. SEM imaging on day 21 confirmed these histological features. Although coarse woven bone was now discernible, it was poorly mineralized and structurally discontinuous. The regenerate lacked cohesive integration with the host bone, further underscoring the suboptimal quality of healing under trace element overload.

DISCUSSION

This study highlights significant differences in the dynamics of cancellous bone healing between physiological conditions and conditions of trace element overconsumption in senile rats. In the control group, the regenerative process followed a classic and orderly sequence of stages – beginning with inflammation, followed by granulation tissue formation, fibroreticular matrix development, and culminating in coarse woven bone deposition by day 21 (Figure 3 (A)). This timeline aligns with established descriptions of fracture healing, in which inflammation and neovascularization are

prerequisites for subsequent bone matrix deposition and mineralization [11, 12].

In contrast, the experimental group, exposed to elevated levels of Zn, Mn, Cu, Pb, and Cr, demonstrated delayed, disorganized, and qualitatively inferior osteogenesis. Although physiological zinc supports osteogenesis, multiple studies show a bi-phasic response: excess Zn^{2+} inhibits osteogenic activity, reduces MSC viability, and perturbs remodeling signaling, potentially compromising bone regeneration [22, 1, 23, 24]. Manganese, like zinc, is essential for bone formation—with a demonstrated ability to promote osteoblast activity and inhibit osteoclastogenesis [25]. However, unlike zinc, there is little evidence that manganese overconsumption directly impairs bone regeneration, although observational data link elevated Mn levels to reduced bone mineral density [26]. While physiological levels support osteogenesis, excessive Cu^{2+} has been shown to exert cytotoxic effects on osteoblasts, reduce alkaline phosphatase activity, and impair collagen synthesis, thereby delaying bone matrix formation and mineralization [27]. Lead is a well-documented bone toxicant that substitutes for calcium in hydroxyapatite, altering crystal structure and reducing mineralization quality [28]. Chronic Pb exposure decreases osteoblast number and function, stimulates osteoclast activity, and suppresses osteocalcin

expression [29]. In contrast to hexavalent chromium, which is acknowledged as toxic and capable of disrupting bone modeling processes [30], there is currently *no experimental evidence* that overconsumption of trivalent chromium (Cr^{3+}) impairs reparative osteogenesis.

The combined overconsumption of these elements resulted in a regenerate on day 21 that comprised not only fibroreticular and coarse woven bone tissue but also a substantial portion ($32.37 \pm 2.59\%$) of cartilaginous tissue. Cartilage formation was only observed at day 21. This presence of cartilage suggests a shift toward endochondral ossification—a deviation from the intramembranous ossification typically observed in metaphyseal bone repair [13]. This observation can be explicitly as an abnormal or compensatory mechanism. This compensatory ossification route is likely triggered by impaired osteoblastic function and disrupted bone matrix formation [31].

The adverse influence of trace element overload on the cellular microenvironment is supported by previous research demonstrating that excessive copper, lead, or zinc can impair osteoblast activity, collagen synthesis, and matrix mineralization [14, 15]. The observed increase in bone marrow adiposity and reduction in osteocyte density further indicate compromised bone viability, consistent with reports of metal-induced oxidative stress and cellular toxicity [32].

Importantly, vascularization – an essential element of bone regeneration – was also detrimentally affected. In the MeG group, both the vascular area and vessel diameter were significantly reduced compared to controls, particularly on day 14, when angiogenesis should peak. Poor neovascularization impairs nutrient delivery, cell migration, and waste clearance, thus stalling progression to mineralized bone formation. Similar findings have been reported in studies exploring the impact of heavy metals on angiogenesis, which show both direct inhibition of endothelial proliferation and indirect suppression via inflammatory pathways [16, 17].

Finally, the findings demonstrate that trace element imbalance can profoundly alter the trajectory of bone healing in aged organisms, reinforcing the need to consider environmental and nutritional factors in managing osteoporotic fractures. These data support the

hypothesis that excessive microelement intake – notably in elderly populations – may contribute to poor fracture outcomes by promoting delayed ossification, impaired angiogenesis, and disrupted cellular signaling.

CONCLUSIONS

This study demonstrates that chronic overconsumption of trace elements, including zinc, copper, manganese, lead, and chromium, profoundly disrupts the normal trajectory of cancellous bone healing in senile rats. In contrast to the orderly and time-dependent sequence of inflammation, granulation, fibroreticular transformation, and woven bone formation observed under physiological conditions, the experimental group exhibited delayed, disorganized, and morphologically inferior regenerative outcomes. In the control group, healing at 7 day progressed with granulation tissue and early vascular formation, though slowed by age-related changes. In contrast, the microelement-overload group showed delayed repair, persistent hematoma, necrosis, and minimal osteogenic activity, reflecting stalled transition from inflammation to regeneration. Notably, by day 14 the regenerate in microelement-overload animals appeared even less organized than at day 7, reflecting a regression in healing dynamics. Moreover, a significant reduction in angiogenic activity was observed, with vessel diameter decreasing from $3.82 \pm 0.6 \mu\text{m}$ in controls to $2.20 \pm 0.24 \mu\text{m}$ in experimental animals at day 14, further hindering osteogenesis. On day 21, instead of mature woven bone as in controls ($62.97 \pm 1.93\%$), the regenerate in the experimental group consisted of $45.76 \pm 0.47\%$ fibroreticular tissue, only $13.6 \pm 0.31\%$ woven bone, and as much as $32.37 \pm 0.74\%$ cartilaginous tissue, indicating a compensatory reliance on endochondral ossification. Therefore, the overloaded group exhibited disorganized remodeling, with fibroreticular tissue, limited woven bone, and substantial cartilage, indicating a pathological shift toward endochondral ossification and impaired angiogenesis. Collectively, the findings underscore the critical importance of trace element homeostasis for successful skeletal repair in aging organisms. This work contributes valuable insights into the pathophysiology of age-related bone regeneration and highlights the potential risks associated with microelemental imbalance in elderly populations.

PROSPECTS FOR FUTURE RESEARCH

The present study provides foundational insights into the detrimental effects of trace element overload on cancellous bone regeneration in senile organisms. However, several questions remain open and warrant further investigation. Detailed profiling of signaling pathways affected by trace elements—particularly those involved in osteogenic differentiation, matrix mineralization, oxidative stress response, and angiogenesis—is essential to elucidate the cellular basis of impaired bone healing.

AUTHOR CONTRIBUTIONS

“Conceptualization, H.L. and O.S.; methodology, H.L. and Y.H.; software, H.L. and Y.H.; validation, I.V., O.S. and H.L.; formal analysis, H.L. and Y.H.; investigation, H.L. and Y.H.; resources, O.S.; data curation, I.V., O.S.; writing—original draft preparation, H.L.; writing—review and editing, O.S.; visualization, H.L. and Y.H.; supervision, I.V., O.S.; project administration, O.S.; funding acquisition, O.S. All authors have read and agreed to the published version of the manuscript.”

FUNDING

This research received no external funding.

CONFLICT OF INTEREST

The authors declare that they have no known competing financial interests or personal relationships that could have influenced the work reported in this paper.

INSTITUTIONAL REVIEW BOARD STATEMENT

Protocols for performing animal experiments were approved by the Ethical Committee of the Sumy State University (Protocol 12/07 from 14.07.2022).

REFERENCES

- Ciosek Ż, Kot K, Rotter I. Iron, Zinc, Copper, Cadmium, Mercury, and Bone Tissue. *Int J Environ Res Public Health*; 20. Epub ahead of print 2023. <https://doi.org/10.3390/ijerph20032197>.
- Alghadir AH, Gabr SA, Al-Eisa ES, et al. Correlation between bone mineral density and serum trace elements in response to supervised aerobic training in older adults. *Clin Interv Aging* 2016; 11: 265–273.
- Coyte RM, Harkness JS, Darrah TH. The Abundance of Trace Elements in Human Bone Relative to Bone Type and Bone Pathology. *GeoHealth*; 6. Epub ahead of print 2022. <https://doi.org/10.1029/2021GH000556>.
- Colón CJP, Molina-Vicenty IL, Frontera-Rodríguez M, et al. Muscle and Bone Mass Loss in the Elderly Population: Advances in diagnosis and treatment. *J Biomed* 2018; 3: 40–49.
- Zofkova I, Davis M, Blahos J. Trace elements have beneficial, as well as detrimental effects on bone homeostasis. *Physiol Res* 2017; 66: 391–402.
- Amhare AF, Liu H, Qiao L, et al. Elemental Influence: The Emerging Role of Zinc, Copper, and Selenium in Osteoarthritis. *Nutrients* 2025; 17: 2069.
- Jomova K, Makova M, Alomar SY, et al. Essential metals in health and disease. *Chem Biol Interact*; 367. Epub ahead of print 2022. <https://doi.org/10.1016/j.cbi.2022.110173>.
- Balali-Mood M, Naseri K, Tahergorabi Z, et al. Toxic Mechanisms of Five Heavy Metals: Mercury, Lead, Chromium, Cadmium, and Arsenic. *Front Pharmacol*; 12. Epub ahead of print 2021. <https://doi.org/10.3389/fphar.2021.643972>.
- Li M, Deng F, Qiao L, et al. The Critical Role of Trace Elements in Bone Health. *Nutr* ; 16. Epub ahead of print 2024. <https://doi.org/10.3390/nu16223867>.
- Wu C, Xiao Y, Jiang Y. Associations of blood trace elements with bone mineral density: a population-based study in US adults. *J Orthop Surg Res*; 18. Epub ahead of print 2023. <https://doi.org/10.1186/s13018-023-04329-9>.
- Li M, Deng F, Qiao L, et al. The Critical Role of Trace Elements in Bone Health. *Nutr* ; 16. Epub ahead of print 2024. <https://doi.org/10.3390/nu16223867>.
- Li G, Cheng T, Yu X. The Impact of Trace Elements on Osteoarthritis. *Front Med*; 8. Epub ahead of print 2021. <https://doi.org/10.3389/fmed.2021.771297>.
- Guo J, Huang X, Dou L, et al. Aging and aging-related diseases: from molecular mechanisms to interventions and treatments. *Signal Transduct Target Ther*; 7. Epub ahead of print 2022. <https://doi.org/10.1038/s41392-022-01251-0>.
- Sandberg OH, Aspenberg P. Inter-trabecular bone formation: a specific mechanism for healing of cancellous bone: A narrative review. *Acta Orthop* 2016; 87: 459–465.
- Romaniuk A, Sikora V, Lyndin M, et al. The features of morphological changes in the urinary bladder under combined effect of heavy metal salts. *Interv Med Appl Sci* 2017; 9: 105–111.
- Clark D, Nakamura M, Miclau T, et al. Effects of Aging on Fracture Healing. *Curr Osteoporos Rep* 2017; 15: 601–608.
- Jukes JM, Both SK, Leusink A, et al. Endochondral bone tissue engineering using embryonic stem cells. *Proc Natl Acad Sci U S A* 2008; 105: 6840–6845.
- Jepsen KJ, Price C, Silkman LJ, et al. Genetic variation in the patterns of skeletal progenitor cell differentiation and progression during endochondral

- bone formation affects the rate of fracture healing. *J Bone Miner Res* 2008; 23: 1204–1216.
19. Ambrosi TH, Scialdone A, Graja A, et al. Adipocyte Accumulation in the Bone Marrow during Obesity and Aging Impairs Stem Cell-Based Hematopoietic and Bone Regeneration. *Cell Stem Cell* 2017; 20: 771–784.e6.
 20. Ye W, Wang Y, Mei B, et al. Computational and functional characterization of four SNPs in the SOST locus associated with osteoporosis. *Bone* 2018; 108: 132–144.
 21. Hu Y, Li X, Zhi X, et al. RANKL from bone marrow adipose lineage cells promotes osteoclast formation and bone loss. *EMBO Rep*; 22. Epub ahead of print 2021. <https://doi.org/10.15252/embr.202152481>.
 22. O'Connor JP, Kanjilal D, Teitelbaum M, et al. Zinc as a therapeutic agent in bone regeneration. *Materials (Basel)*; 13. Epub ahead of print 2020. <https://doi.org/10.3390/ma13102211>.
 23. Park KH, Park B, Yoon DS, et al. Zinc inhibits osteoclast differentiation by suppression of Ca²⁺-Calcineurin-NFATc1 signaling pathway. *Cell Commun Signal*; 11. Epub ahead of print 2013. <https://doi.org/10.1186/1478-811X-11-74>.
 24. Murni NS, Dambatta MS, Yeap SK, et al. Cytotoxicity evaluation of biodegradable Zn-3Mg alloy toward normal human osteoblast cells. *Mater Sci Eng C* 2015; 49: 560–566.
 25. Taskozhina G, Batyrova G, Umarova G, et al. The Manganese–Bone Connection: Investigating the Role of Manganese in Bone Health. *J Clin Med*; 13. Epub ahead of print 2024. <https://doi.org/10.3390/jcm13164679>.
 26. Wang C, Zhu Y, Long H, et al. Relationship between blood manganese and bone mineral density and bone mineral content in adults: A population-based cross-sectional study. *PLoS One*; 17. Epub ahead of print 2022. <https://doi.org/10.1371/journal.pone.0276551>.
 27. Glenske K, Donkiewicz P, Köwitsch A, et al. Applications of metals for bone regeneration. *Int J Mol Sci*; 19. Epub ahead of print 2018. <https://doi.org/10.3390/ijms19030826>.
 28. Ellis DE, Terra J, Warschkow O, et al. A theoretical and experimental study of lead substitution in calcium hydroxyapatite. *Phys Chem Chem Phys* 2006; 8: 967–976.
 29. Carmouche JJ, Puzas JE, Zhang X, et al. Lead exposure inhibits fracture healing and is associated with increased chondrogenesis, delay in cartilage mineralization, and a decrease in osteoprogenitor frequency. *Environ Health Perspect* 2005; 113: 749–755.
 30. Sánchez LM, Ubios ÁM. Hexavalent chromium exposure alters bone remodeling in the developing tooth alveolus and delays tooth eruption. *Acta Odontol Latinoam* 2021; 34: 91–97.
 31. Meyers C, Lisiecki J, Miller S, et al. Heterotopic Ossification: A Comprehensive Review. *JBMR Plus*; 3. Epub ahead of print 2019. <https://doi.org/10.1002/jbm4.10172>.
 32. Chandra A, Lagnado AB, Farr JN, et al. Bone Marrow Adiposity in Models of Radiation- and Aging-Related Bone Loss Is Dependent on Cellular Senescence. *J Bone Miner Res* 2022; 37: 997–1011.

Received 12.05.2025

Accepted 23.09.2025

INFORMATION ABOUT THE AUTHORS

Lohvyniuk H. – PhD student Department of Oncology and Radiology Medical Institute Sumy State University, Sumy, Ukraine.

Husak Y. – PhD student of the Joint Program between Silesian University of Technology, Poland and Sumy State University, Ukraine.

Vynnychenko I. – PhD in Medicine, Associate Professor, Head of the Department of Surgery and Oncology Medical Institute of the Sumy State University

Solodovnyk O. – PhD, assistant of the Department Of Surgery, Traumatology, Orthopedics And Phthisiology.